An Efficient Nonlinear Backstepping Controller Approach of a Wind Power Generation System Based on a DFIG

Sara Mensou*‡, Ahmed Essadki*, Tamou Nasser**, Badr Bououlid Idrissi***

* Electrical Engineering Department of ENSET, Mohammed V University, BP 6207 Rabat, Morocco

** Communication Networks Department of ENSlAS, Mohammed V University, BP 713 Rabat, Morocco

*** Electromechanical Engineering Department of ENSAM, Moulay Ismaïl University, BP 4024 Meknes, Morocco

(sara.mensou11@gmail.com, ahmed.essadki1@gmail.com, tnasser@ensias.ma, bbououlid@yahoo.fr)

‡ Corresponding Author; Sara Mensou, Electrical Engineering Department of ENSET, Mohammed V University, Rabat Morocco, Tel: +212 644 641 77, sara.mensou11@gmail.com

Received: 26.02.2017 Accepted:12.03.2017

Abstract-In this paper; we present an efficient and robust nonlinear control model for wind energy conversion system based on a doubly fed induction generator (DFIG). The aim of this work is to develop a model, which combines the vector control and the nonlinear Backstepping approach to control the currents rotor and the mechanical rotor speed of the generator in order to extract the maximum of the power produced. The robustness and performance of the system are tested and compared with classical PI controller in terms of reference tracking whatever generator parameters variations. Simulation results were evaluated and presented under MATLAB/SIMULINK Software.

Keywords DFIG, Wind turbine, MPPT, Backstepping Controller, Lyapunov function.

1. Introduction

At the beginning of the 21st century, the exploitation and development of renewable energy resources, especially wind turbine, becomes the priority of several countries. The reasons for this interest in wind conversion system technologies are the bulk availability of this resource without any cost and it's the most environmental means to get electricity from an inexhaustible source [1-2].

Various researches have focused in the study of wind power generation systems using doubly fed induction generator (DFIG) from an endless source [2-6]. The most used machine in the wind farms is the doubly fed induction generator, the stator of the generator is connected directly to a phase grid and the rotor is connected to the utility grid via a two power converters linked by a DC bus (Fig.1) [7-8]. This structure has several advantages such as; allows operation at over a large range of wind speeds of about ± 30% around the synchronous speed which allows to better exploit the resources wind turbines, and the power converters are sized to use a fraction (25%-30%) of the total power produced by the generator to achieve full control of the system, Consequently, the reduction of losses in power electronics components [7], [9].

The Control of the doubly fed induction generator is more difficult than the control of a standard induction machine. Various control methods have been developed in the literature [10-13]. The classical control for DFIG used PI controller is the most applied in industrial applications for his good reliability, easy maintenance and low cost, but when the internal parameters of the system are subject to changes caused by physical phenomena the classical PI controller performances may be changed [14].

These recent decades, many studies have focused on the nonlinear controller such us Backstepping control which has

enjoyed perfect success for his robustness against disturbance and simplicity of implementation [15].

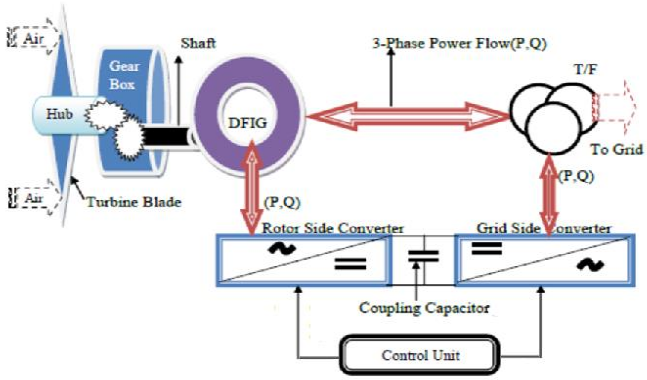

Fig.1. Diagram of the wind energy system based on the DFIG.

The purpose of this work is to advance an efficient nonlinear control design which combines the Backstepping method and the vector control for controlling the DFIG, in order to vary the mechanical speed of the generator for each wind speed to provide the maximum of the electrical power produced. To show the importance of this study, the proposed control strategy was compared with the classical PI controller used in each to improve the system robustness and stability. The results obtained by simulation under Matlab/Simulink environment prove the robustness of the control model in terms of stability, dynamic performance, effectiveness and the reference tracking against parameter variations of the generator.

This paper is presented as follows; the second section is devoted to the mathematical model of the wind turbine and the principle of MPPT control (Maximum Power Point Tracking). In the third section we introduce the modeling of the generator in the Park reference (d-q). The description of mathematical development of the proposed nonlinear approach is detailed in Section 4. In the fifth section, we present numerical simulation results, we discuss and we compare with those of the PI controller for illustrating the control effectiveness and the performance of our study. Finally, we provide some conclusions.

2. Modelling of the Wind Turbine

The extracted power from the wind turbine is written as follows[16]:

$$P_{\upsilon} = \frac{\rho.S.v^3}{2} \quad (1)$$

Wind turbines transform the mechanical energy generated by the wind to the electrical energy. The aerodynamic power available on the rotor is expressed as follows [17-20]:

$$P_{aer} = C_p(\lambda.\beta).P_{\upsilon} \quad (2)$$

$$P_{aer} = C_p(\lambda.\beta).\frac{\rho.S.v^3}{2} \quad (3)$$

Where ρ, S, v, C_p, λ et β are the air density (ρ=1.22 kg/m3), the circular surface swept by the turbine, the wind speed, the power coefficient, speed ratio and the pitch angle of the blade, respectively.

The expression $C_p(\lambda.\beta)$ defines the aerodynamic efficiency of the wind turbine; it depends on the blade pitch angle β and the speed ratio λ, which is defined as [21-22]:

$$\lambda = \frac{R.\Omega_t}{v} \quad (4)$$

The aerodynamic torque is given by :

$$T_{aer} = \frac{P_{aer}}{\Omega_t} = C_p(\lambda.\beta).\frac{\rho.S.v^3}{2.\Omega_t} \quad (5)$$

The power coefficient $C_p(\lambda.\beta)$ can be described as follows [23]:

$$C_p(\lambda.\beta) = 0.5176(\frac{116}{\lambda_i} - 0.4\beta - 5)e^{-\frac{21}{\lambda_i}} + 0.0068\lambda \quad (6)$$

$$\lambda_i = \frac{1}{\lambda + 0.008.\beta} - \frac{0.035}{\beta^3 + 1} \quad (7)$$

The characteristics of $C_p(\lambda.\beta)$ depending of λ for different values of β are presented in the Fig.2.

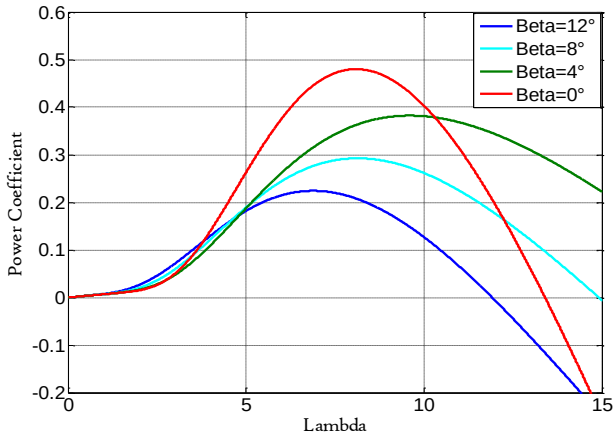

Fig. 2. Aerodynamic Power Coefficient $C_p(\lambda.\beta)$

From the Figure 2 we found that the maximum value of C_p is $C_{p\max}$ = 0.48, which corresponds to the pitch angle of the blade $\beta = 0°$ and the optimum speed ratio λ_{opt} = 8.1. By setting β and λ respectively to their optimal values, the wind system will provide optimum electrical power.

The multiplier adjusts the slow speed of the rotation of the turbine to the high mechanical speed of the generator; this multiplier is modelled by a gain G. The total inertia J depends on the inertia of the generator J_g on the fast axis and the inertia of the turbine J_t on the slow axis [18].

$$J = \frac{J_t}{G^2} + J_g \quad (8)$$

The fundamental equation of dynamics makes it possible to determine the evolution of the mechanical speed from the total mechanical torque T_{mec} is given by [7]:

$$J\frac{d\Omega_{mec}}{dt} = T_{mec} = T_g - T_{em} - C_f.\Omega_{mec} \quad (9)$$

Where:

T_g : The generator torque.

T_{em} : The electromagnetic torque.

$C_f.\Omega_{mec}$: The torque of viscous friction.

3. MPPT Control

The aim of this control is to optimize the capture wind energy by tracking the optimal speed, to extract the maximum of the power produced from the wind turbine; we must always adjust the rotor speed of the generator to the wind speed [18]. In order to estimate the value of the wind speed which gives the maximum of the power we can fixed the speed ratio λ to its optimum value λ_{opt} that corresponds to the maximum power coefficient $C_{p\max}$ (Fig.3). According to equation 4 it's can be possible to deduce in real time the estimate value of the wind speed:

$$v_{est} = \frac{R.\Omega_t}{\lambda_{opt}} \quad (10)$$

The expression of the reference electromagnetic torque as a function of the mechanical speed is expressed as [24]:

$$T_{em\,ref} = \frac{1}{2}C_{p\max}(\lambda.\beta).\frac{\rho.\pi.R^5}{(G.\lambda_{opt})^3}\Omega_{mec}^{\ 2} \quad (11)$$

The block diagram in Fig.3 shows the model of the turbine and the MPPT control.

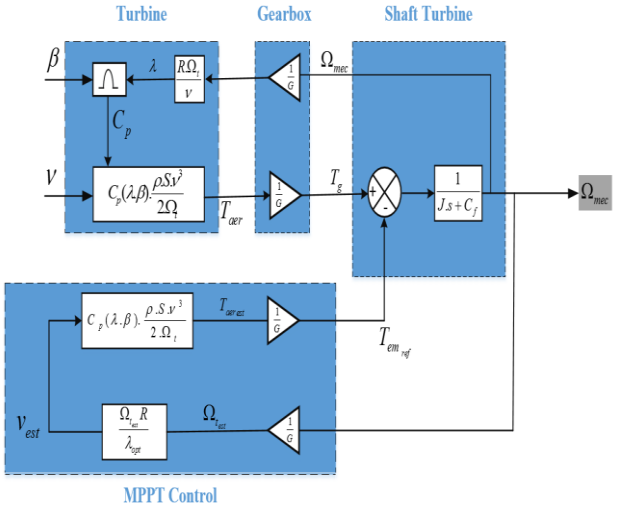

Fig. 3. Schematic diagram of the Turbine model and MPPT control.

4. Modeling of the DFIG

4.1. Mathematical Model of the DFIG

The general mathematical model of the doubly fed induction generator in the Park reference (d-q) is given by the following equations [8], [15]:

$$\begin{cases} V_{sd} = R_s.I_{sd} + \dfrac{d\varphi_{sd}}{dt} - \varphi_{sq}.\omega_s \\ V_{sq} = R_s.I_{sq} + \dfrac{d\varphi_{sq}}{dt} + \varphi_{sd}.\omega_s \\ V_{rd} = R_r.I_{rd} + \dfrac{d\varphi_{rd}}{dt} - \varphi_{rq}.\omega_r \\ V_{rq} = R_r.I_{rq} + \dfrac{d\varphi_{rq}}{dt} + \varphi_{rd}.\omega_r \end{cases} \quad (12)$$

$$\begin{cases} \varphi_{sd} = L_s.I_{sd} + L_m.I_{rd} \\ \varphi_{sq} = L_s.I_{sq} + L_m.I_{rq} \\ \varphi_{rd} = L_s.I_{rd} + L_m.I_{sd} \\ \varphi_{rq} = L_r.I_{rq} + L_m.I_{sq} \end{cases} \quad (13)$$

Where ω_s is the pulsation of the currents stator and ω_r is the pulsation of the currents rotor, is given by:

$$\omega_r = \omega_s - p.\Omega \quad (14)$$

Where p is the number of the pole pairs of an induction machine.

$R_s; R_r$: The stator and rotor resistance

$L_{s.}; L_r$: The cyclic stator and rotor inductance

L_m : The mutual inductance

The electromagnetic torque of the DFIG is expressed as:

$$T_{em} = \frac{3}{2}.p.\frac{L_m}{L_s}.(\varphi_{sq}.I_{rd} - \varphi_{sd}.I_{rq}) \quad (15)$$

The stator and rotor active and reactive powers of the DFIG are expressed as follows [18]:

$$\begin{cases} P_s = V_{sd}.I_{sd} + V_{sq}.I_{sq} \\ Q_s = V_{sq}.I_{sd} - V_{sd}.I_{sq} \\ P_r = V_{rd}.I_{rd} + V_{rq}.I_{rq} \\ Q_r = V_{rq}.I_{rd} - V_{rd}.I_{rq} \end{cases} \quad (16)$$

4.2. Vector control

The use of the asynchronous machine can adopt several types of control such as vector control, which is ensures decoupling between his variables and making it similar to a DC generator [25].

In our study, we chose a park reference (d-q) linked to the rotating field. Assuming that the flux stator is constant and oriented along the axis d of the rotating reference frame and the stator resistance R_s is neglected [7], the equations of

the stator voltages and flux can be simplified as follow [18], [26]:

$$\begin{cases} \varphi_{sd} = L_s.I_{sd} + L_m.I_{rd} = \varphi s \\ \varphi_{sq} = L_s.I_{sq} + L_m.I_{rq} = 0 \\ V_{sd} = R_s.I_{sd} + \dfrac{d\varphi_{sd}}{dt} - \varphi_{sq}.\omega_s = 0 \\ V_{sq} = R_s.I_{sq} + \dfrac{d\varphi_{sq}}{dt} + \varphi_{sd}.\omega_s = \varphi s.\omega_s \\ V_{rd} = R_r.I_{rd} + (L_r - \dfrac{L_m^{\,2}}{L_s}).\dfrac{dI_{rd}}{dt} - \omega_r.(L_r - \dfrac{L_m^{\,2}}{L_s}).I_{rq} \\ V_{rq} = R_r.I_{rq} + (L_r - \dfrac{L_m^{\,2}}{L_s}).\dfrac{dI_{rq}}{dt} + \omega_r.(L_r - \dfrac{L_m^{\,2}}{L_s}).I_{rd} + \omega_r.\dfrac{L_m}{L_s}.\varphi s \end{cases} \quad (17)$$

The expression of the electromagnetic torque can be expressed:

$$T_{em} = -\frac{3}{2}.p.\frac{L_m}{L_s}.\varphi s.I_{rq} \quad (18)$$

The simplified expressions for the active and reactive powers of the stator are written as follows:

$$P_s = -\frac{V_s.L_m}{L_s}.I_{rq} \quad (19)$$

$$Q_s = \frac{V_s.\varphi s}{L_s} - \frac{V_s.L_m}{L_s}.I_{rd} \quad (20)$$

The schematic diagram of the simplified model of the DFIG in Park reference (d-q) is shown in Fig.4.

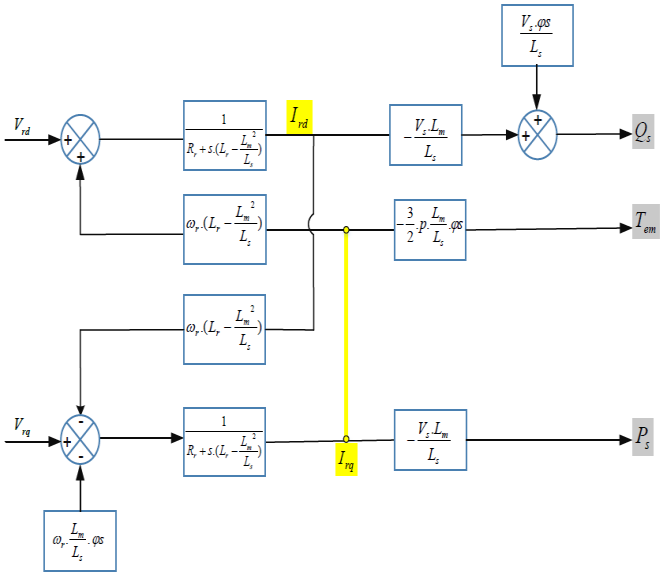

Fig. 4. Block diagram of the DFIG in the Park reference (d-q).

5. Backstepping Controller

The Backstepping approach is a recursive controldesign for stabilizing highly nonlinear dynamic systems [27]. The principle of the Backstepping controller approach is the use of a virtual control to decompose a complex nonlinear design problem into various simpler design steps. The stability andperformance of the system are achieved by using a Lyapunov function which is used to drive the virtual control [15].

According to equation (8), (16) and (17), the equations of the DFIG become:

$$\begin{cases} \dfrac{dI_{rd}}{dt} = -b.I_{rd} + \omega_r.I_{rq} + a.V_{rd} = g_1 + a.V_{rd} \\ \dfrac{dI_{rq}}{dt} = -b.I_{rq} - \omega_r.I_{rd} - c.\varphi s.\omega_r + a.V_{rq} = g_2 + a.V_{rq} \end{cases} \quad (21$$

$$) \frac{d\Omega}{dt} = \frac{T_g}{J} - \frac{c_f}{J}.\Omega + \frac{d}{J}.I_{rd} \quad (22)$$

Where:

$$\begin{cases} g_1 = -b.I_{rd} + \omega_r.I_{rq} \\ g_2 = -b.I_{rq} - \omega_r.I_{rd} - c.\varphi s.\omega_r \\ \sigma = 1 - \dfrac{L_m^{\,2}}{L_s.L_r}; a = 1 - \dfrac{1}{\sigma.L_r}; b = a.R_r; c = a.\dfrac{L_m}{L_s}; d = -\dfrac{3}{2}p.\dfrac{L_m}{L_s}.\varphi s \end{cases} \quad (23)$$

According to Eq. (21) and Eq. (22), we concluded that V_{rd} and V_{rq} are the variables of the rotor voltages to impose on the machine in order to achieve the currents rotor and the mechanical speed desired. The scheme presented in Fig.5 is the proposed model control of the DFIG by the Backstepping controller.

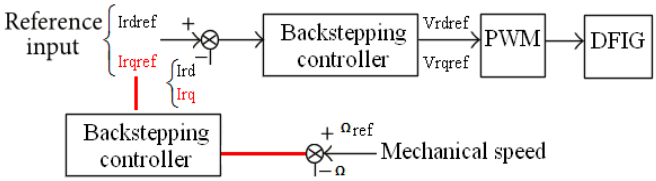

Fig. 5. Block diagram of the proposed Backstepping controller.

5.1. *The Calculation of the Reference Current Rotor* I_{rq}

The mechanical speed tracking error e_1 is defined by:

$$e_1 = \Omega_{ref} - \Omega \quad (24)$$

The derivative of the equation (24) gives:

$$\dot{e}_1 = \dot{\Omega}_{ref} - \dot{\Omega} \quad (25)$$

Using Eq. (21) the previous equation becomes as the following form:

$$\dot{e}_1 = \dot{\Omega}_{ref} - (\frac{T_g}{J} - \frac{C_f}{J}.\Omega + \frac{d}{J}.I_{rq}) \quad (26)$$

To reduce the tracking error, we use the following first Lyapunov function [23]:

$$v_1 = \frac{1}{2}e_1^{\,2} \quad (27)$$

Using the equation (26) and (27) the derivative of the first Lyapunov function v_1 is given by:

$$\dot{v}_1 = e_1.\dot{e}_1 = e_1.(\dot{\Omega}_{ref} - \frac{T_g}{J} + \frac{C_f}{J}.\Omega - \frac{d}{J}.I_{rq}) = -k_1.e_1^{\,2} \quad (28)$$

In order to guarantee a stable tracking, k_1 should be positive parameter [14]. From Eq. (28), the expression of the control variable I_{rq} can be rewritten as:

$$I_{rq\,ref} = \frac{J}{d}.(\dot{\Omega}_{ref} + k_1.e_1) + \frac{1}{d}.(C_f.\Omega - T_g) \quad (29)$$

5.2. The calculation of the reference rotor voltages V_{rd} and V_{rq}

The currents rotor tracking errors e_2 and e_3 are defined by:

$$\begin{cases} e_2 = I_{rdref} - I_{rd} \\ e_3 = I_{rqref} - I_{rq} \end{cases} \quad (30)$$

The derivative of equation (29) gives:

$$\begin{cases} \dot{e}_2 = \dot{I}_{rdref} - \dot{I}_{rd} \\ \dot{e}_3 = \dot{I}_{rqref} - \dot{I}_{rq} \end{cases} \quad (31)$$

Using equation (21), (22) and (31), we get:

$$\begin{cases} \dot{e}_2 = \dot{I}_{rdref} - (g_1 + a.V_{rd}) \\ \dot{e}_3 = \dot{I}_{rqref} - (g_2 + a.V_{rq}) = \frac{J}{d}.(\ddot{\Omega}_{ref} + k_1.\dot{e}_1) + \\ \frac{1}{d}.(C_f.\dot{\Omega} - \dot{T}_g) - (g_2 + a.V_{rq}) \end{cases} \quad (32)$$

To reduce the tracking error, we use a new Lyapunov candidate function, such that [23]:

$$v_2 = \frac{1}{2}e_1^{\,2} + \frac{1}{2}e_2^{\,2} + \frac{1}{2}e_3^{\,2} \quad (33)$$

Using the equation (32) and (33), the derivative of v_2 is given by:

$$\dot{v}_2 = e_1.\dot{e}_1 + e_2.\dot{e}_2 + e_3.\dot{e}_3 \quad (34)$$

$$\dot{v}_2 = -k_1.e_1^{\,2} - k_2.e_2^{\,2} - k_3.e_3^{\,2} + e_2.(k_2.e_2 + \dot{I}_{rdref} - g_1 - a.V_{rd}) + e_3(k_3.e_3 + \frac{J}{d}.(\ddot{\Omega}_{ref} + k_1.\dot{e}_1) + \frac{1}{d}.(C_f.\dot{\Omega} - \dot{T}_g) - g_2 - a.V_{rq}) \quad (35)$$

Where k_2 and k_3 should be positives in order to guarantee a good and stable tracking [14]. Using the Eq. (26) and (35) the expressions of the control variables V_{rd} and V_{rq} are expressed by:

$$\begin{cases} V_{rdref} = \frac{\dot{I}_{rdref} - g_1 + k_2.e_2}{a} \\ V_{rqref} = \frac{\mu - k_1.I_{rqref} - g_2 + k_3.e_3}{a} \end{cases} \quad (36)$$

With:

$$\mu = \frac{1}{d}.(J.\ddot{\Omega}_{ref} + k_1.(J.\dot{\Omega}_{ref} - T_g + C_f.\Omega) + C_f.\dot{\Omega} - \dot{T}_g) \quad (37)$$

That ensure $\dot{v}_2 \le 0$. The performance and the stability the of the system are giving by a good choice of k_1, k_2 and k_3.

6. Simulation Results and Discussions

The simulation of the whole system is performed using the MATLAB/Simulink software. The values of the system parameters are given respectively in the appendix. The Table 1. present the Backstepping controller parameters are chosen to satisfy the convergence conditions.

Table 1. Backstepping controller parameters

Symbol	Value
k_1	0.002
k_2	100
k_3	200

6.1. Reference Tracking and Control

We apply a random wind profile, which varies between 8 m/s and 11 m/s. It shows clearly in Fig.6. From Fig.7 that, the mechanical speed extracting from the MPPT controller varies in the same shape as the wind speed.

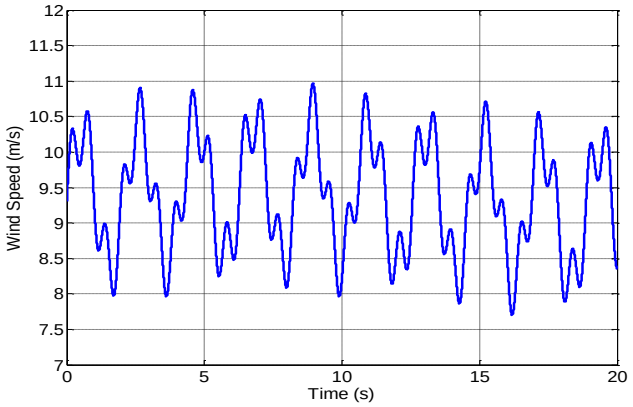

Fig. 6. Wind Speed (m/s).

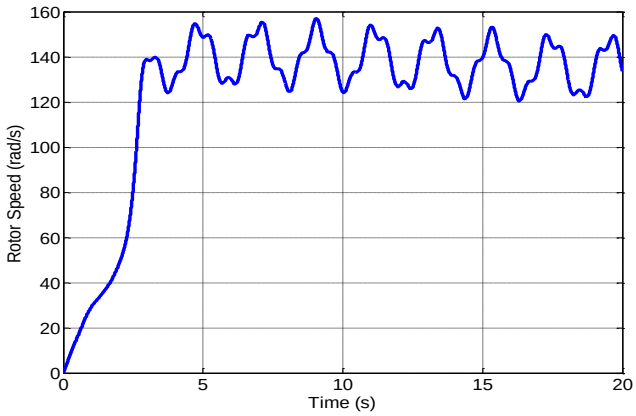

Fig. 7. Reference Mechanical Speed extracted from the MPPT control.

Furthermore, comparing Fig.8 with Fig.9, we notice that the rotor currents I_{rd} and I_{rq} follow perfectly their reference values and the decoupling between them is well assured. The rotor current I_{rd} shown in Fig.8 is kept a constant value to have a unity power factor on the stator side to optimize the quality of the energy produced [18]. The response of the current rotor I_{rq} that controls the mechanical speed of the generator is shown in Fig.9. The variation of I_{rq} is following the wind speed variation in order to extract the maximum of the electrical power generated. The tracking profile is depicted in Fig.10 shows the rotor speed varies in accordance with its reference speed. It is seen that the Backstepping control lead to good tracking performance.

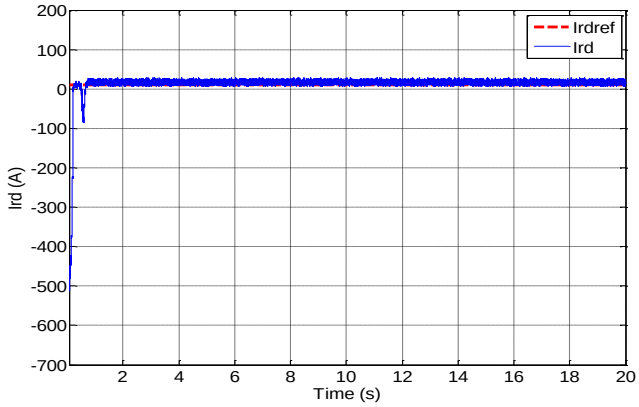

Fig. 8. Rotor Current I_{rd} and its reference.

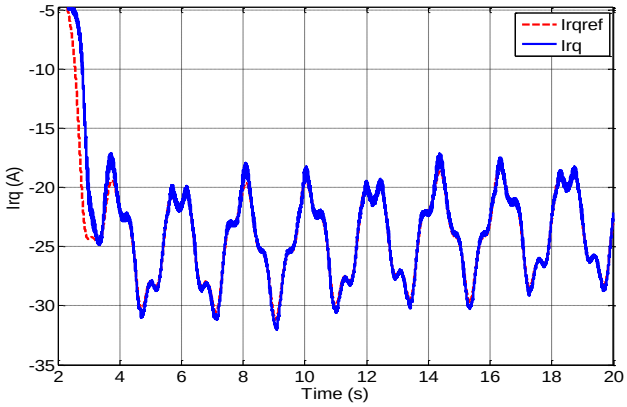

Fig. 9. Rotor Current I_{rq} and its reference.

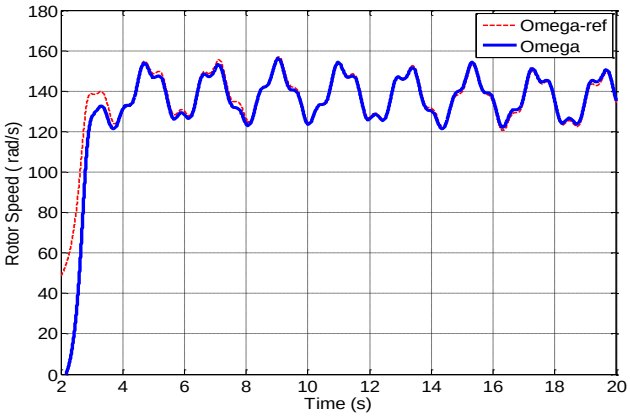

Fig. 10. Mechanical Speed and its reference.

From the Fig.11, it can be seen that the stator active power is negative Ps<0 and it varies between -4000 W and -10 KW, although of this change, the power coefficient C_p keeps at its maximum value $C_{p\max}$ = 0.48 (show Fig.12), which confirm the robustness of the MPPT control. Scanning the simulation results, we concluded that MPPT control and Backstepping approach are efficient and robust.

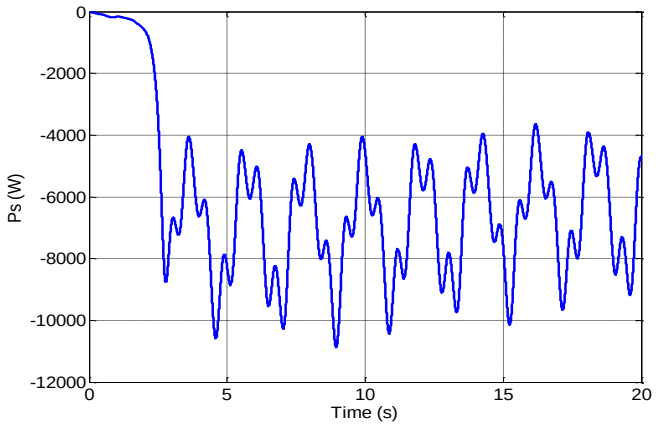

Fig. 11. Stator Active Power.

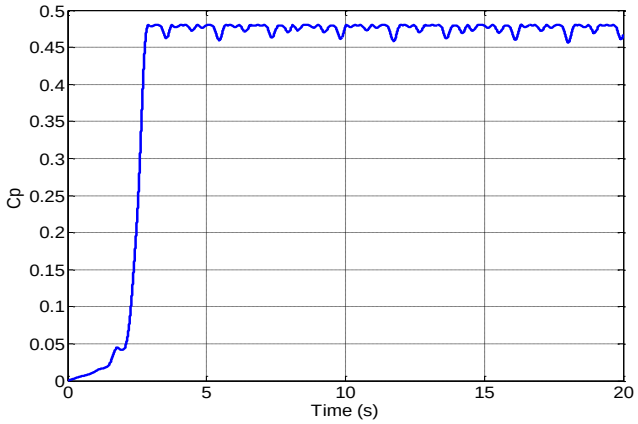

Fig. 12. Power Coefficient.

6.2. Robustness Test

The internal parameters of the DFIG are subject to variations caused by different physical phenomena such as the temperature increase, saturation and skin effect, so our controller must provide good results whatever generator parameters variations.

The robustness of the Backstepping controller is proved by comparing the results with those of PI controller in terms of reference tracking when we varied the internal generator parameters.

Figures 13 and 14 illustrate the evolution of the current rotor I_{rq} after the variation of rotor resistance and inductance from Rr to 2Rr and Lr to 2Lr respectively. This variation has almost no influence on Backstepping controller and the tracking of the set point is always ensured. However by using the PI controller, with the same performance, this variation shows more undesirable responses.

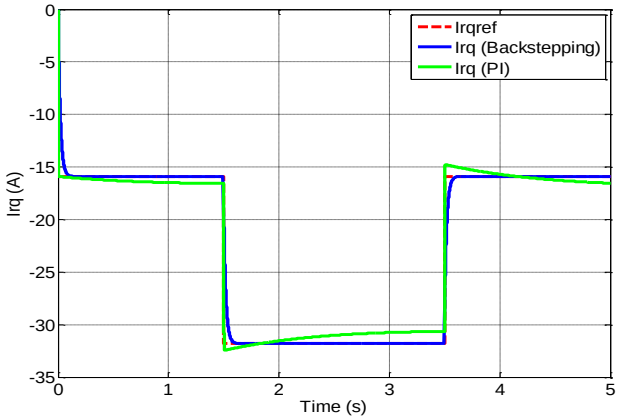

Fig. 13. Current Rotor I_{rq} and its reference after variation of the rotor resistance.

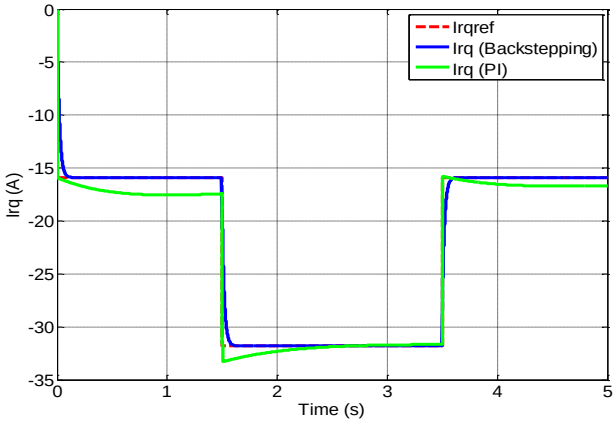

Fig. 14. Current Rotor I_{rq} and its reference after variation of the rotor inductance.

7. Conclusion

This paper describes an efficient and robust control of DFIG applied in a wind system by using the nonlinear Backstepping controller, MPPT strategy. After modeling the generator in the Park reference (d-q), we have adopted a vector control of the DFIG based on stator flux oriented to decouple the control of direct and quadrature currents rotor. In addition, we are interested in modeling of various components of wind system. To validate the proposed control model of the system, we have performed a simulation in Matlab/Simulink. Finally, we have compared our model to the classical PI controller in terms of reference tracking when we change the DFIG internal parameters.

According to the simulation results, the Backstepping approach ensured with better efficiency and robustness the control of the mechanical rotor speed and the currents rotor of the generator, which allows operation of the wind energy system at the maximum of the electrical power produced to the network.

Appendix: Characteristics and Parameters

Table 2. DFIG Parameters

Denotation	Numerical value of parameter
Rated Power	$P = 10KW$
Nominal frequency	$f = 50Hz$
Number of pole pair	$p = 2$
Stator resistance	$R_s = 0.455\Omega$
Rotor resistance	$R_r = 0.62\Omega$
Stator inductance	$L_s = 0.084\,H$
Rotor inductance	$L_r = 0.085\,H$
Mutual inductance	$L_m = 0.078\,H$

Table 3. Wind Turbine Parameters

Denotation	Numerical value of parameter
Radius of the turbine	$R = 3m$
Gain multiplier	$G = 5.4$
Inertia total moment	$J = 0.2kg.\mathrm{m}^2$
Coefficient of viscous friction	$C_f = 0.0024m/s$
Optimal tip speed ratio	$\lambda_{opt} = 8.1$
Maximal power coefficient	$C_{p\max} = 0.48$

References

[1] A.D. Sahin, "Progress and Recent Trends in Wind Energy", Progress in Energy and Combustion Science, vol. 30, pp. 501-543, 2004.

[2] B. Beltran, T. Ahmed Ali, M. Benbouzid, "Sliding mode power control of variable speed wind energy conversion systems", IEEE Transl. Energy Conversion, vol. 23, pp. 551-558, June 2008.

[3] B. Boukhezzar and H. Siguerdidjane, "Nonlinear control with wind estimation of a DFIG variable speed wind turbine for power capture optimization", Energy Conversion and Management, vol. 50, pp. 885-892, 2009.

[4] A.G. Abo-Khalil, "Synchronization of DFIG output voltage to utility grid in wind power system", Renewable Energy, vol. 44, pp. 193-198, 2012.

[5] F. Poitiers, T. Bouaouiche and M. Machmoum, "Advanced control of a doubly-fed induction generator for wind energy conversion", Electric Power Systems Research, vol. 79, pp. 1085-1096, 2009.

[6] Z. Song, T. Shi, C. Xia and W. Chen, "A novel adaptive control scheme for dynamic performance improvement of DFIG-Based wind turbines", Energy, vol. 38, pp. 104-117, 2012.

[7] R. Chakib, A. Essadki, M. Cherkaoui, "Active Disturbance Rejection Control for Wind System Based On a DFIG", International Journal of Electrical Computer Energetic Electronic and Communication Engineering, vol. 8, pp. 1306-1315, 2014.

[8] A. Boualouch, A. Frigui, T. Nasser, A. Essadki, A. Boukhriss, "Control of a Doubly-Fed Induction Generator for Wind Energy Conversion Systems by RST Controller", International Journal of Emerging Technology and Advanced Engineering, vol. 4, pp. 93-99, August 2014.

[9] R. Datta and V. Ranganathan, "Variable-Speed Wind Power Generation Using a Doubly Fed Wound Rotor Induction Machine: A Comparison with Alternative Schemes", IEEE Power Engineering Review, vol. 22, pp. 52-55, Jul 2002.

[10] L. Yang, Z. Xu, J. Ostergaard and ZY. Dong, "Advanced Control Strategy of DFIG Wind Turbines for Power System Fault Ride Through", IEEE Transactions on Power Systems, vol. 27, pp. 713-722, 2012.

[11] C. Belfedal, S. Moreau, G. Champenois, T. Allaoui and M. Denai, "Comparison of PI and Direct Power Control with SVM of Doubly Fed Induction Generator", Journal of Electrical & Electronics Engineering, vol 8, pp. 633-641, 2008.

[12] J. Ben Alaya, A. Khedher and M. F. Mimouni, "DTC and Nonlinear Vector Control Strategies Applied to the DFIG operated at Variable Speed", WSEAS Transactions on environment and development, vol. 6, pp. 744-753, 2010.

[13] J. Ben Alaya, A. Khedher and M. F. Mimouni, "DTC, DPC and Nonlinear Vector Control Strategies Applied to the DFIG operated at Variable Speed", Journal of Electrical Engineering JEE, vol. 6, pp. 744-753, 2011.

[14] A. Khedher, A. Khemiri, M. F. Mimouni," Wind Energy Conversion System using DFIG controlled by Backstepping and Sliding Mode Strategies". International Journal of Renewable Energy Research, vol. 2, pp. 421-430, 2012.

[15] A. Boualouch, A. Essadki, T. Nasser, A. Boukhriss, A. Frigui, "Power Control of DFIG in WECS Using Backstipping and Sliding Mode Controller", International Journal of Electrical Computer Energetic Electronic and Communication Engineering, vol. 9, pp. 612-618, 2015.

[16] I. Nouira, A. Khedher, A. Bouallegue. "A Contribution to the Design and the Installation of an Universal Platform of a Wind Emulator using a DC

Motor". International Journal of Renewable Energy Research, vol. 2, pp. 797-804, 2012.

[17] S. F. Panah, T. F. Panah, G. A. Ghannad. "Reactive Power Compensation in Wind Power Plant with Short Circuit in Power Plant Line via UPFC". Proc. 5thIEEE Conf. on Renewable Energy Research and Applications, Birmingham UK, pp. 173-176, Nov 2016.

[18] R. Chakib, A. Essadki, M. Cherkaoui, "Modeling and Control of a Wind System based on a DFIG by Active Disturbance rejection control", International Review on Modeling and Simulations, vol. 7, pp. 626-637, August 2014.

[19] D. R. Rush and G. W. David, "Nonlinear Power Flow Control Design", Springer, New York, NY, USA, 2011.

[20] M.L. Corradini, G. Ippoliti, G. Orlando, "An Aerodynamic Torque Observer for the Robust Control of Variable-Speed Wind Turbines", Proc. 51st IEEE Conf. on Decision and Control, pp. 2483-2488, Maui, Hawaii, USA, 10-13 December 2012.

[21] K. E. Okedu, "Effects of drive train model parameters on a variable speed wind turbine". International Journal of Renewable Energy Research, vol. 2, pp. 92-98, 2012.

[22] Y. Soufi, S. Kahla, M. Sedraoui & M. Bechouat. "Optimal Control based RST Controller for Maximum Power Point Tracking of Wind Energy Conversion System". Proc. 5thIEEE Conf. on Renewable Energy Research and Applications, Birmingham UK, pp. 1168-1172, Nov 2016.

[23] M. Rachidi, B. B. Idrissi, "Robust Nonlinear Backstepping Control Design for Doubly Fed Induction Machine in Wind Power Generation", International Journal of Research in Engineering & Advanced Technology, vol. 3, pp. 137-145, Feb-Mar 2015.

[24] C. Z. El Archi, T. Nasser, A. Essadki, "Power Control of DFIG Based Wind System: Comparison between Active Disturbance Rejection Controller and PI Controller", ARPN Journal of Engineering and Applied Sciences, vol. 11, pp. 13980-13989, December 2016.

[25] Z. Mekrini, S. Bri, "Performance of an Indirect Field Oriented Control for Asynchronous Machine", International Journal of Engineering and Technology, vol. 8, pp. 726-733, Apr-May 2016.

[26] K. Ghedamsi, E.M. Berkouk, "Control of Wind Generator Associated to a Flywheel Energy Storage System", Renewable Energy, Elsevier, vol. 33, pp. 2145-2156, 2008.

[27] F. Ikhouane, M. Krstc, "Robustness of the Tuning Functions Adaptive Backstepping Design for Linear Systems", IEEE Transl. Automat. Contr., vol. 43, pp. 431-437, 1998.